Research Paper

Ripk3 induces mitochondrial apoptosis via inhibition of FUNDC1 mitophagy in cardiac IR injury

Hao Zhou[a,*,1], Pingjun Zhu[a,1], Jun Guo[a,1], Nan Hu[b], Shuyi Wang[b], Dandan Li[a], Shunying Hu[a], Jun Ren[b], Feng Cao[a], Yundai Chen[a,**]

[a] Department of Cardiology, Chinese PLA General Hospital, Beijing, China
[b] Center for Cardiovascular Research and Alternative Medicine, University of Wyoming College of Health Sciences, Laramie, WY 82071, USA

ARTICLE INFO

ABSTRACT

Ripk3-required necroptosis and mitochondria-mediated apoptosis are the predominant types of cell death that largely account for the development of cardiac ischemia reperfusion injury (IRI). Here, we explored the effect of Ripk3 on mitochondrial apoptosis. Compared with wild-type mice, the infarcted area in Ripk3-deficient (Ripk3^{-/-}) mice had a relatively low abundance of apoptotic cells. Moreover, the loss of Ripk3 protected the mitochondria against IRI and inhibited caspase9 apoptotic pathways. These protective effects of Ripk3 deficiency were relied on mitophagy activation. However, inhibition of mitophagy under Ripk3 deficiency enhanced cardiomyocyte and endothelia apoptosis, augmented infarcted area and induced microvascular dysfunction. Furthermore, ischemia activated mitophagy by modifying FUNDC1 dephosphorylation, which substantively engulfed mitochondria debris and cytochrome-c, thus blocking apoptosis signal. However, reperfusion injury elevated the expression of Ripk3 which disrupted FUNDC1 activation and abated mitophagy, increasing the likelihood of apoptosis. In summary, this study confirms the promotive effect of Ripk3 on mitochondria-mediated apoptosis via inhibition of FUNDC1-dependent mitophagy in cardiac IRI. These findings provide new insight into the roles of Ripk3-related necroptosis, mitochondria-mediated apoptosis and FUNDC1-required mitophagy in cardiac IRI.

1. Introduction

Reperfusion itself results in additional damage, known as cardiac ischemia-reperfusion injury (IRI) [1]. During reperfusion, the death of cardiomyocytes [2] and cardiac microvascular endothelia cells [3] (CMECs) are the key factors that determine the disease course and prognosis. Necrosis and apoptosis are the two major cell death mechanisms in IRI [4]. Over the past years, necroptosis is determined to be the prominent mode of programmed cell death (PCD) in response to IRI via the Ripk1/Ripk3/MLKL pathways [4–6]. Interestingly, many studies have suggested that necroptosis has multiple interactions in apoptosis [7,8]. Ripk1 is the upstream signal of caspase8-mediated apoptosis [9], but activated caspase 8 degrades Ripk3 and inhibits subsequent necroptosis [10]. Whether the disruption of Ripk3 could aggregate or alleviate apoptosis remains unclear.

Mitophagy is also a protective mechanism enabling the efficient and selective elimination of damaged mitochondria to attenuate mitochondria-mediated apoptosis via the engulfment of ruptured mitochondria and neutralization of pro-apoptotic factors [11]. However, no information is available about the fundamental relationship between Ripk3 and mitophagy in cardiac IRI. Considering the regulatory role of mitophagy in apoptosis [12–14], we propose that shared signaling pathway elements between apoptosis and necroptosis may be involved in mitophagy. Furthermore, mitophagy could be activated via PINK/ Parkin pathways and FUNDC1 pathways according to previous studies [15,16]. As for the PINK/Parkin, little solid evidence is available for the role of Parkin in cardiac IRI when compared with FUNDC1. Furthermore, the activator of Parkin is PINK which locates in the mitochondria but not in the cytoplasm [17]. However, Ripk3 is a cytoplasmic protein which has the kinases property (for example, Ripk3 could induce the MLKL phosphorylation modification) [18]. Based on such two reasons, we think that Parkin may not be indirectly regulated by Ripk3. On the other hand, FUNDC1 is the receptor of LC3II and locates on the surface of mitochondria outer membrane [19]. Moreover, several studies have

indicated the protective role of FUNDC1 in cardiac IRI [15]. Meanwhile, FUNDC1 could be inactivated or activated via phosphorylation modification [20]. These information hint that Ripk3 has the ability to regulate mitophagy via FUNDC1. Thus, in the present study, using loss- and gain-of-function experiments related to Ripk3 in vitro and in vivo, we observed that Ripk3 deficiency suppressed cellular apoptosis. Specifically, upregulated Ripk3 during reperfusion disrupted ischemia-induced mitophagy via the post-transcriptional modification of FUNDC1, committing cells to mitochondria-mediated apoptosis and amplifying cardiac myocytes and microvascular reperfusion injury.

2. Methods

2.1. Animal and ex vivo models of cardiac reperfusion injury

All protocols were approved by the PLA General Hospital Institutional Animal Care and Use Committee. Ripk3$^{-/-}$ mice with a C57BL/6 background were generated as previously described [21]. Ripk3$^{-/-}$ and wild-type (WT) male mice (12-wk-old) underwent a procedure to induce cardiac IRI according to our previous studies. A 7-0 silk suture was placed around the left anterior descending coronary artery, and a reversible slipknot was tied for 30 min and subsequently loosened for 2 h for reperfusion. Then, blood samples were collected for analysis of LDH, Troponin T and CK-MB levels. The hearts (n = 6/group) were used for infarct size measurement using 2% Evans blue and 1% TTC.

2.2. Cardiomyocyte and CMEC isolation, experimental groups and reperfusion injury induction in vitro

Cardiomyocytes and CMECs were isolated from the hearts of Ripk3$^{-/-}$ and WT mice using the enzyme dissociation method as described by our previous studies [22,23]. For experimental groups in vitro, cardiomyocytes and CMECs were obtained from WT and Ripk3$^{-/-}$ mice, named the WT and Ripk3$^{-/-}$ groups, respectively. In addition, Ripk3 gain-of-function experiments (Ad + Ripk3$^{-/-}$) were performed by Ripk3 adenovirus vector overexpression in cells isolated from Ripk3$^{-/-}$ mice. Reperfusion injury was mimicked in vitro according to our previous study [24]. Hypoxia was conducted in a 37 °C airtight chamber saturated with 95% N_2/5% CO_2 for 30 min with H-DMEM/serum starvation, and reoxygenation was performed in a 37 °C/5% CO_2 incubator under H-DMEM/10% FBS for 2 h. To trigger mitophagy, FCCP (5 μm) was added for 120 min to induce mitophagy according to previous study [25]. To inhibit mitophagy, 3-MA (10 mM) was pretreated for 2 h.

2.3. Echocardiogram and microvascular imaging using gelatin-ink perfusion

Echocardiography was performed by echocardiogram (14.0 MHz, Sequoia C512; Acuson, Germany) to observe the change of cardiac function (n = 6/group) according to our previous study [26].

The 37 °C ink plus 3% gelatin (gelatin-ink staining via the jugular vein) was applied for gelatin-ink perfusion after a 2-h reperfusion. Rapid ligature of the great vessel of the cardiac base and the superior and inferior vena cava was performed once the limbs appeared black. Then, the heart was maintained at 4 °C for at least 1 h to promote gelatin coagulation. Thereafter, the heart was fixed in 4% paraformaldehyde and processed for cryosectioning.

2.4. Immunohistochemistry and immunofluorescence staining

The following primary antibodies were used for immunohistochemistry and immunofluorescence staining: Ripk3 (1:200), TOMM20 (1:1000), LC3II (1:500), F-actin (1:1000), Tubulin (1:1000), all from Abcam, USA. DAPI (Sigma-Aldrich, USA), lysosome stain (Abcam, USA) and a mitochondrion-selective MitoFluor™ stain

(Molecular Probes, USA) were used to detect the nuclei, lysosomes and mitochondria, respectively.

2.5. Mitochondrial membrane potential (ΔΨm) measurement, mitochondrial permeability transition pore (mPTP) opening evaluation and mitochondrial ROS (mROS) detection

The ΔΨm was visualized using the JC-1 Kit (Beyotime, China) and the mPTP opening was assessed as the rapid dissipation of tetramethylrhodamine ethyl ester (TMRE) fluorescence according to our previous study [27]. The arbitrary mPTP opening time was determined as the time when TMRE fluorescence intensity decreased to halfway between the initial and residual fluorescence intensity. The mROS was detected using a MitoSOX™ Red Mitochondrial Superoxide Indicator (Molecular Probes, USA), observed using a microscope or analyzed by flow cytometry.

2.6. Caspase3/9 activity, LDH release and TUNEL assays

Caspase3/9 activity (Beyotime, China), LDH release (Beyotime, China) and TUNEL late-apoptotic (Roche Applied Bio Sciences, USA) analyses were performed using commercial kits as previously described [28].

2.7. Trypan blue staining and MTT assay for cellular death evaluation

Trypan blue is a vital stain used to selectively color dead cells blue. After treatment, the cells were treated with 0.4% trypan blue. Then, trypan blue-positive cell images were acquired and analyzed using a fluorescence microscope. MTT was conducted in a 96-well plate in triplicate. After reperfusion injury, 20 μl of MTT (5 mg/ml PBS, pH 7.4) was added, and the plate was incubated for another 4 h. The supernatant was subsequently discarded, and 100 μl of DMSO was added to each well for 10 min. Finally, the optical density (OD) value was measured at A490 nm, reflecting cell viability according to our previous study [23].

2.8. Migration assay

The migration assay of CMECs was evaluated using 24-well transwell chamber (Coring, U.S.A.) according to our previous study [22]. Firstly, 10^5 CMECs were seeded in the upper chamber in serum-free medium. The chemotactic agent SDF-1 (Sigma-Aldrich, U.S.A., 100 ng/ml) was added to the lower chamber to induce CMEC migration. After 12 h incubation at 37 °C, non-migrating cells in the upper chamber were carefully removed with cotton swab, cells that had traversed the membrane were fixed in methanol, stained with 0.05% crystal violet.

2.9. Calcium imaging

After treatment, cardiomyocytes were placed on a glass coverslip and were incubated with 1 μM Fura-2/AM for 30 min at room temperature. After washing three times with PBS to remove extracellular dye, the coverslip was fixed in in the Warner model RC-26 chamber (Warner Instruments, Hamden, CT, USA) and PH-1 heated platform (Warner Instruments, Hamden, CT, USA). Then cells were observed on an inverted microscope (Olympus America, Melville, NY, USA) and Fura-2 fluorescence was alternately excited at the wavelengths of 340 nm and 380 nm with a monochromater (TILL Photonics, Polychrome V, Munich, Bavaria, Germany). Intracellular free calcium concentration was calculated according to the previous study [29].

2.10. Western blot analysis and co-immunoprecipitation

The following primary antibodies were used for western blot analyses: caspase3 (1:1000), caspase9, (1:1000), caspase12 (1:1500),

caspase8 (1:1000) and PARP (1:1000) were purchased from Abcam; MLKL (1:1000), cytochrome c (1:1000), p-MLKL (p-358) (1:1000), p-Drp (S616) (1:1000) and p-Drp1 (S637) (1:1000) were purchased from Cell Signaling Technology. Anti-p-FUNDC1 (Tyr18) (1:500) and anti-FUNDC1 (1:1,1000) polyclonal antibodies were produced by immunizing rabbits with synthesized and purified phosphorylated and non-phosphorylated peptides from FUNDC1 (Abgent, SuZhou, China) according to a previous study [15,30,31].

Coimmunoprecipitation experiments were performed as our previous study described. Briefly, proteins from cells were cross-linked in 1% paraformaldehyde followed by washing in PBS containing 100 mmol/L glycine. The cells were then lysed by sonication in PBS with 1% Triton X-100 and incubated with the respective antibodies and

protein A/G agarose. The immunoprecipitates were loaded on a SDS-PAGE and probed with FUNDC1 antibody.

2.11. Electron microscopy

For electron microscopy, the samples were dehydrated using acetonitrile and graded methanol, embedded in epoxy resin (EMbed-812; Electron Microscopy Sciences, USA) and polymerized at 70 °C overnight. A Hitachi H600 Electron Microscope (Hitachi, Japan) was used to capture the images.
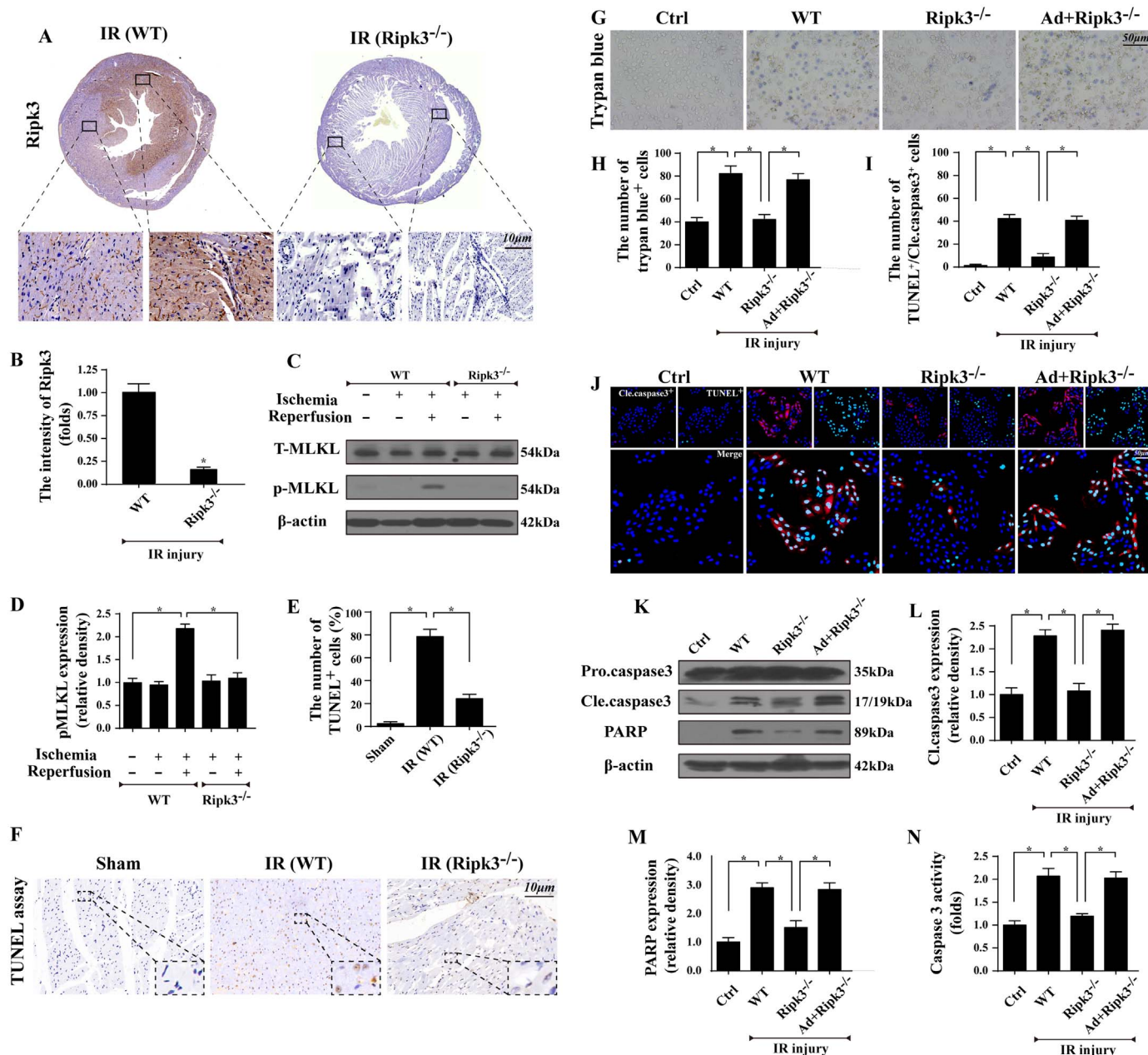
Fig. 1. The role of Ripk3 in apoptosis in response IRI. Cardiac IRI was conducted by 30 min of ischemia followed by 2 h of reperfusion in vivo and 30 min of hypoxia and 2 h of reoxygenation (n = 6/group). **A–B.** The change of Ripk3 tended to increase in the infarct area relative to the baseline via immunohistochemistry. **C–D.** The p-MLKL was upregulated at the stage of reperfusion but not in the period of ischemia. **E–F.** TUNEL assay indicated that loss of Ripk3 caused less TUNEL positive cells in infarcted heart. **G–H.** Loss of Ripk3 reduced the number of trypan blue positive cells in cardiomyocytes. **I–J.** TUNEL and cleaved caspase3 co-staining were used to assess the apoptosis rate of cardiomyocytes when Ripk3 was deficiency. **K–M.** The expression of pro-caspase3, cleaved caspase3 and PARP in Ripk3 deficiency. N. The quantitative analysis about the role of Ripk3 deficiency in caspase3 activity during IRI in cardiomyocytes. *P < 0.05.

2.12. Construction of adenovirus (AD) for Ripk3 overexpression

For Ripk3 overexpression, the pDC316-mCMV-Ripk3 plasmid was purchased from Vigene Bioscience and subsequently transfected with a framework plasmid (1:1) into 293 T cells using Lipofectamine 2000. After transfection for 48 h, the viral supernatant was collected and identified by PCR. Following amplification, the supernatant was acquired again and filtered through a 0.45-μm filter to obtain Ad-Ripk3.

The transfection efficiency results were presented in supplemental Fig. 1A-B. Compared to the Ripk3$^{-/-}$ cells, overexpression of Ripk3 via adenovirus increased the contents of Ripk3 about ~2.5 folds.

2.13. Statistical analyses

The data are presented as the mean ± standard deviation (SD) of at least three independent experiments and analyzed by one-way analysis
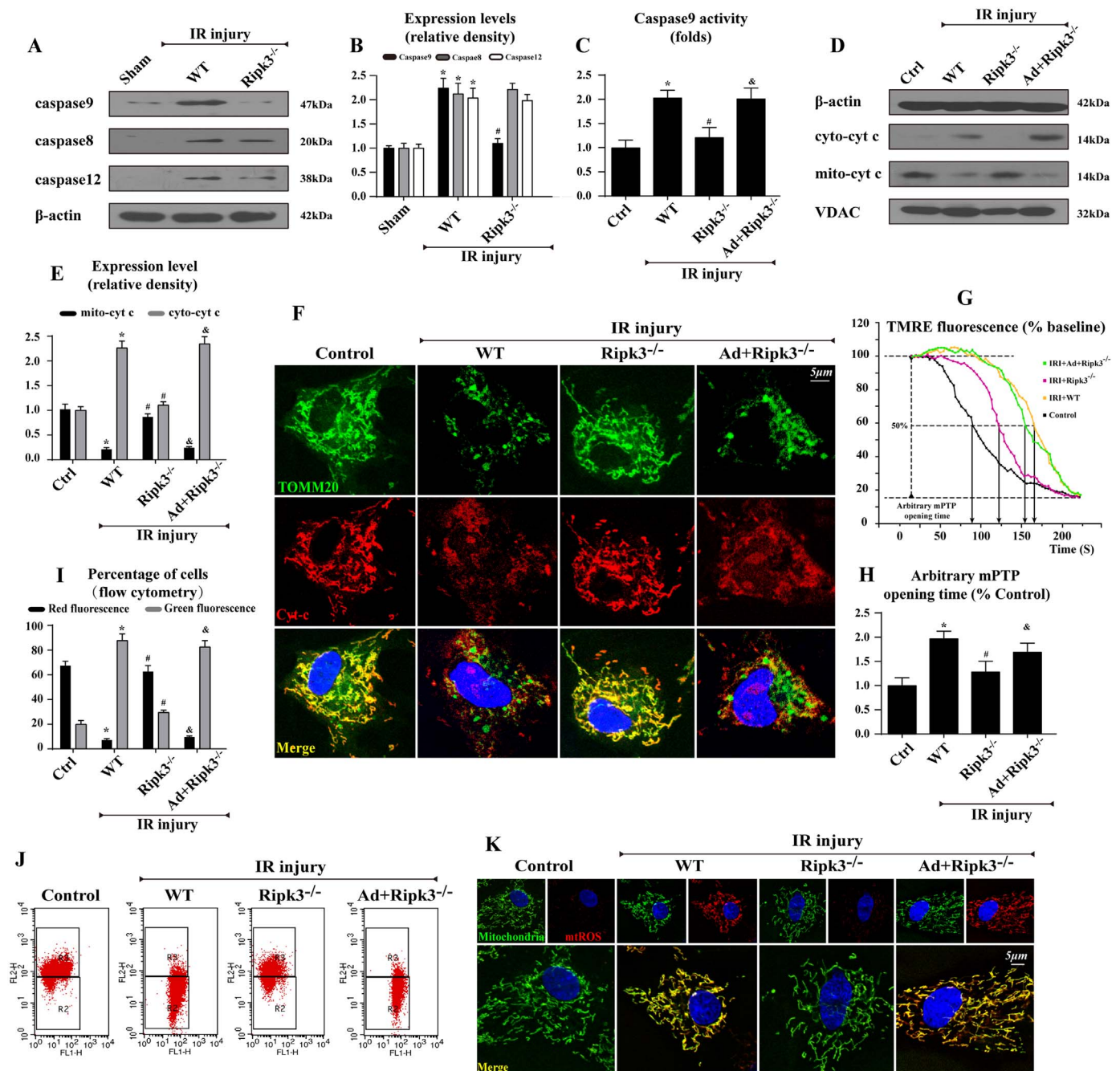
Fig. 2. Ripk3 exacerbates the damage to mitochondria, leading to cyt-c leakage into the cytoplasm, mROS outburst and caspase9 activation. WT mice- and RIPK3$^{-/-}$ mice-derived cardiomyocytes were named WT and Ripk3-/- group, respectively. Furthermore, Ripk3 gain-of-function experiments was performed in cardiomyocytes from Ripk3 using adenovirus vector (Ad+Ripk3$^{-/-}$ group). The IRI in vitro was mimicked by 30 min of hypoxia and 2 h of reoxygenation. **A-B**. The changes of caspase12, caspase8 and caspase9 in response to Ripk3 deficiency under IRI. **C**. Loss of Ripk3 reduced caspase9 activity. **D-E**. Less cyt-c released form mitochondria if knockdown of Ripk3 in cardiomyocytes. **F**. The co-location of cyt-c and mitochondria in cardiomyocytes. In normal cells, cyt-c was characterized by punctate appearance in mitochondria. However, IRI resulted in diffusion of cyt-c from mitochondria into cytoplasm even translocated into nuclear but Ripk3 deficiency could inhibit such effect. **G-H**. Arbitrary mPTP opening time was shorten via TMRE fluorescence when Ripk3 was lost in cardiomyocytes. Arbitrary mPTP opening time was determined as the time when the TMRE fluorescence intensity decreased by half between the initial and residual fluorescence intensity. **I-J**. The ΔΨm was visualized via JC-1 staining in cardiomyocytes. In flow cytometry analysis, R$_2$ and R$_3$ regions represented distribution of green (damaged mitochondria) and red fluorescence (healthy mitochondria) respectively. **K**. Ripk3 induced mROS outburst in response to IRI. *P < 0.05 vs the sham group; #P < 0.05 vs the wild-type (WT) group, &P < 0.05 vs the Ripk3$^{-/-}$ group.
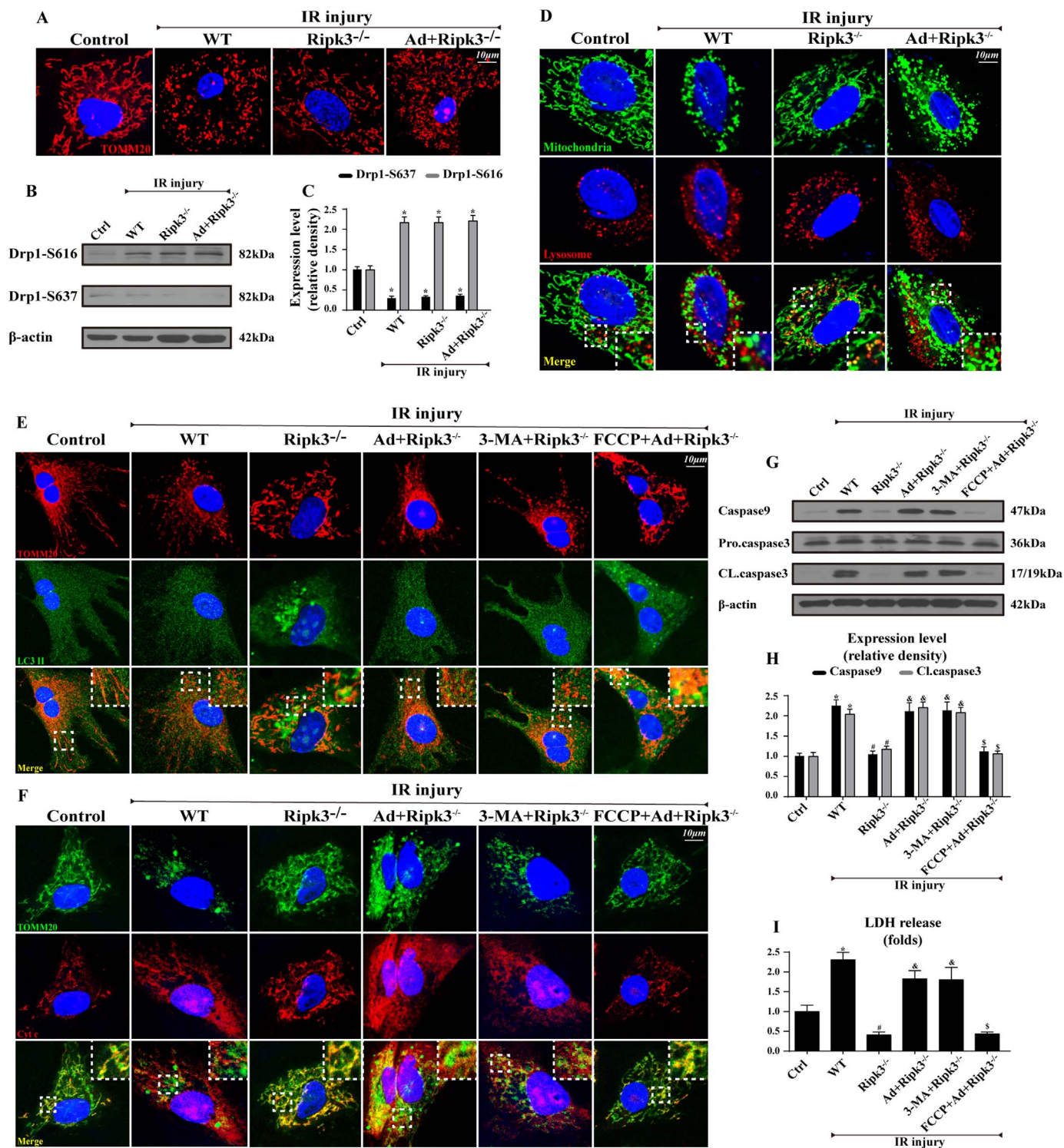
Fig. 3. Increased Ripk3 was associated with inactivate mitophagy, leading to the accumulation of damaged mitochondria and apoptosis activation. **A.** Fragmented mitochondria were observed in IRI but decreased after the loss of Ripk3 in cardiomyocytes. **B-C.** IRI activated Drp1 via post-transcriptional phosphorylation regulation and on change was observed after Ripk3 silencing or overexpression. **D.** The co-immunofluorescence of lysosome and mitochondria in cardiomyocytes. Loss of Ripk3 could activate mitophagy as evidenced by fragmented mitochondria containing in lysosome, ultimately recovering tubular mitochondria. **E.** The co-location of LC3II and mitochondria in cardiomyocytes. Loss of Ripk3 could induce the accumulation of LC3II which was cancelled by Ripk3 overexpression, suggesting the inhibitory effect of Ripk3 on LC3II activation. **F.** Increased mitophagy was associated with less cyt-c diffusion into cytoplasm in cardiomyocytes. **G-H.** The change of caspase9 and caspase3 expression in cardiomyocytes suggested that Ripk3 deletion could alleviate caspase9-related mitochondrial apoptosis via increasing mitophagy. **I.** Mitophagy also reduced LDH release. *P < 0.05 vs the control group; #P < 0.05 vs the wild-type (WT) group, & P < 0.05 vs the Ripk3$^{-/-}$ group, $P < 0.05 vs the Ad + Ripk3$^{-/-}$ group.

of variance (ANOVA). The limit of statistical significance between the treated and control groups was P < 0.05.

3. Results

3.1. Loss of Ripk3 reduces total cell death and the percentage of apoptosis

Firstly, Ripk3 expression tended to increase in the infarct area (figure A-B) relative to the baseline. Moreover, compared with the sham group, the expression Ripk3 downstream, p-MLKL was increased in reperfusion stage rather than in the period of ischemia, which were decreased in Ripk3$^{-/-}$ mice (Fig. 1C–D). Moreover, to explore the role of Ripk3 in apoptosis, TUNEL assay was used. IRI greatly increased the number of TUNEL$^+$ cells in infarcted heart. Surprisingly, the phenotype was rescued by the deletion of Ripk3 (E–F). In vitro, loss of Ripk3 not

only has the ability to lessen total cell death via trypan blue assay (G–H) but also reduce cellular apoptosis as evidenced by less number of TUNEL$^+$/cleaved caspase3$^+$ cells (I–J), down-regulated caspase3/ PARP expression (K–M) and reduced caspase3 activity (N) in cardio-myocytes. However, once regain of Ripk3, an obvious increase trend in the cell apoptosis appeared. Besides, the pro-apoptotic effect of Ripk3 was also found in CMECs via LDH release (Supplemental Fig. 2A) and caspase3 expression (Supplemental Fig. 2B–C). These data indicated that termination of Ripk3 could decrease the proportion of cellular apoptosis in response to IRI.

3.2. Ripk3 deficiency blocks caspase9-dependent mitochondrial apoptotic pathways

Next, we focused on the upstream change of caspase3. There were
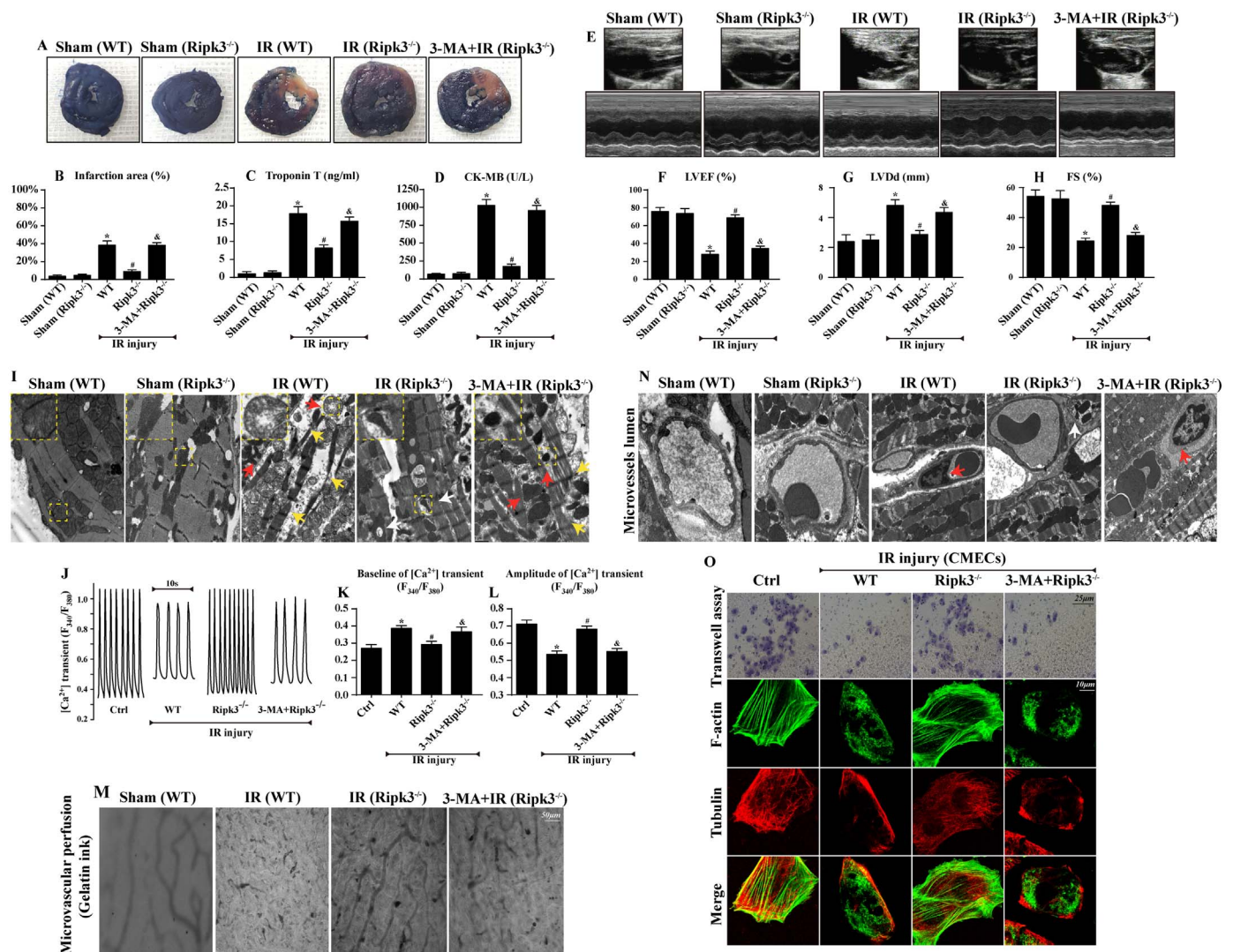
Fig. 4. Ripk3 contributed to infarcted area expansion and cardiac/microvascular dysfunction via the suppression of mitophagy. Cardiac IRI was conducted by 30 min of ischemia followed by 2 h of reperfusion in vivo (n = 6/group) and 30 min of hypoxia and 2 h of reoxygenation. **A.** Representative images of infarcted size via TTC and Evans Blue staining. **B.** Bar graph indicated the infarct size expressed as a percentage of the total left ventricular area. **C–D.** The change of Troponin T contents and CK-MB values. **E-H.** Representative M-mode echo-cardiograms was performed after 2 h reperfusion with the parasternal long-axis view in each group. Quantitative analysis of cardiac function by echocardiography. **I.** The TEM was used to observe the structure change of the infarcted area in vivo. Yellow arrow: myocyte dissolution or muscular fiber twisting and Z line disappearance, red arrow: damaged and swollen mitochondria, white arrow: mitophagy (mitochondria contained in lysosome). **J.** Representative tracings of F_{340}/F_{380} fluorescence ratio. **K.** [Ca^{2+}]i transient baseline. **L.** Amplitude of [Ca^{2+}]i transient. Data are presented as the mean ± SEM (n = 6, for each group). **M.** Microvascular image detection by ink staining. **N.** TEM was used to observe the structural changes of microvessel in response to IRI, including microvascular wall destruction or luminal stenosis (red arrow) and mitophagy (whit arrow). **O.** The CMEC migration response to SDF-1 was analyzed by performing a transwell assay. IRI could reduce the mobility of CMECs via inhibition of mitophagy by up-regulation of Ripk3. Furthermore, the co-immunofluorescence of F-actin and Tubulin indicated that the collapse of migration-related proteins in response to Ripk3 overexpression or mitophagy inhibition. *P < 0.05 vs the sham group (in vivo) or control group (in vitro), #P < 0.05 vs the wild-type (WT) group, &P < 0.05 vs the Ripk3$^{-/-}$ group. FS indicates fractional shortening; LVDd, left ventricular diastolic dimension; LVEF, left ventricular ejection fraction.

no alterations in the ER-involved caspase12 or the Fas-associated caspase8 in response to the loss of Ripk3 (Fig. 2A–B). Notably, the expression (Fig. 2A–B) and activity (Fig. 2C) of mitochondria-associated caspase9 were decreased under Ripk3 deficiency. Caspase9 is activated by the pro-apoptotic factors (such as cyt-c) leakage from damaged mitochondria via mPTP. While our data demonstrated that Ripk3 deficiency limited cyt-c translocation from the mitochondria to the cytoplasm through WB (Fig. 2D–E) and immunofluorescence (Fig. 2F) in cardiomyocytes. Moreover, the time of mPTP opening was reduced (Fig. 2G–H), the ΔΨm was stabilized (Fig. 2I–J) and the mROS overproduction was alleviated (Fig. 2K) in Ripk3-depleted cells but these effects were dramatically reversed by Ripk3 overexpression. Additionally, caspase9 activity (Supplemental Fig. 3A), cyt-c detainment (Supplemental Fig. 3B–C), ΔΨm sustainment (Supplemental Fig. 3D–E) and mROS production (Supplemental Fig. F–G) in CMECs were also consistent with the results in cardiomyocytes. Collectively, this information suggested that Ripk3 deficiency blocked mitochondria-induced apoptosis.

3.3. Ripk3 causes fragmented mitochondria accumulation, reflecting its inhibitory actions on mitophagy

The activation of mitochondrial apoptosis was closely associated with the morphological change of mitochondria [32]. Our data demonstrated that the IRI produced mitochondrial fragmentations in cardiomyocytes (Fig. 3A) and CMECs (Supplemental Fig. 4A), and this effect was alleviated by Ripk3 knockdown. Mitochondrial fragmentation is primarily dependent on Drp1-evoked fission [33] and unexpectedly, there was no causal relationship between the Ripk3 level and conformational change in Drp1 phosphorylation regardless of cardiomyocytes (Fig. 3B–C) or CMECs (Supplemental Fig. 4B–C). Thus, the inability of Ripk3 deficiency to trigger Drp1-evoked fission raised the question of how Ripk3 deficiency reduces mitochondrial disruption [34].

Mitochondrial debris were derived from fission but could be removed by mitophagy [35]. IRI slightly promoted an overlap between the lysosome and mitochondria in cardiomyocytes (Fig. 3D) or CMECs (Supplemental Fig. 4D). However, the lack of Ripk3 significantly
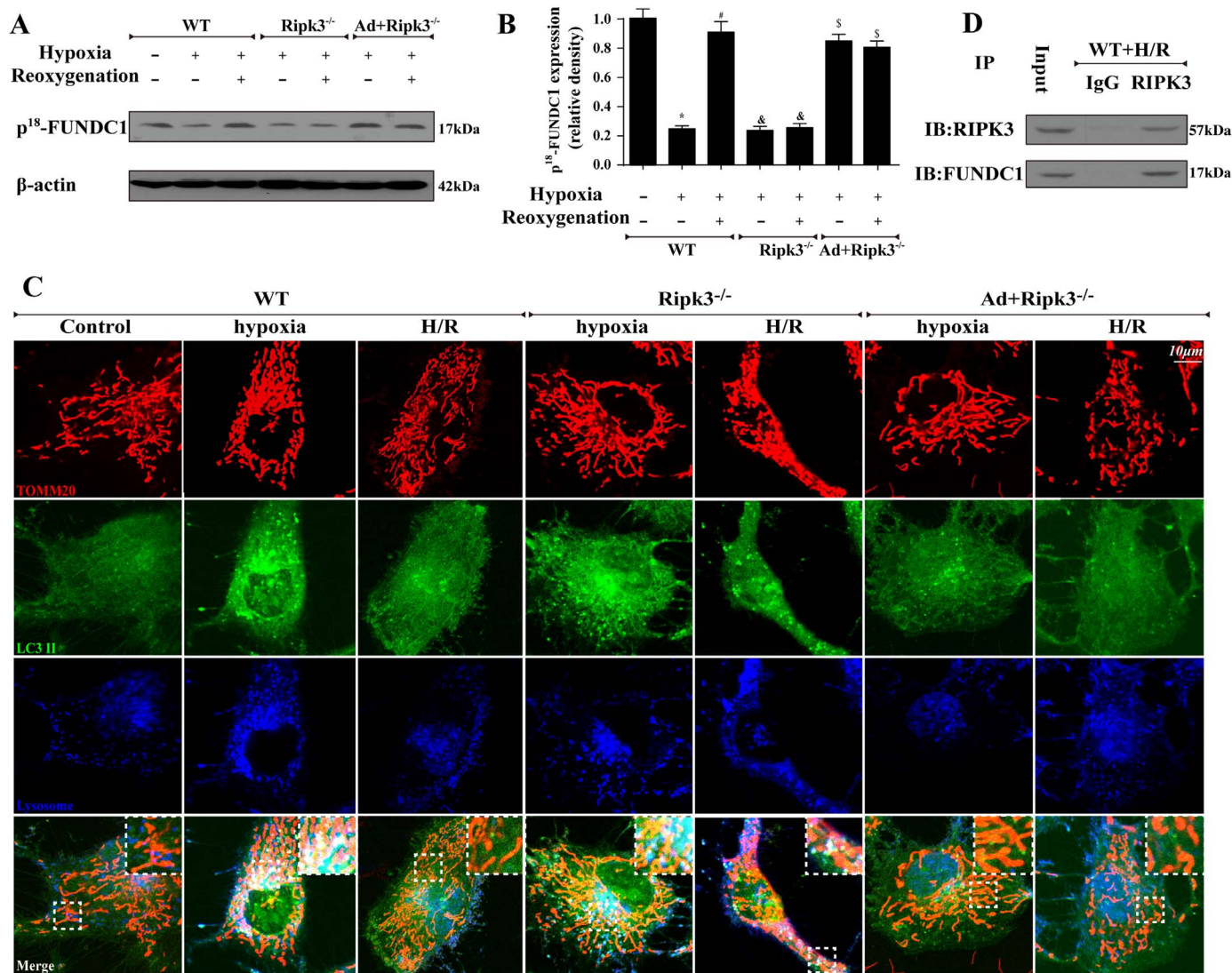
Fig. 5. Ischemia activated FUNDC1-required mitophagy which was inhibited in reperfusion stage due to the increased Ripk3 in cardiomyocytes. **A–B.** The different change of FUNDC1 at hypoxia and reoxygenation phase. Hypoxia activated FUNDC1 via dephosphorylation at Tyr18 but reoxygenation inactivated FUNDC1 via phosphorylation modification. Loss of Ripk3 at reoxygenation phase could reverse FUNDC1 activity. However, overexpression of Ripk3 could significantly limit the FUNDC1 dephosphorylated activation regardless of hypoxia or reoxygenation stimulation. **C.** The co-staining of LC3II, mitochondria and lysosome. Hypoxia-mediated the overlap of mitochondria, LC3II and lysosome was inhibited by reoxygenation. However, loss of Ripk3 at reoxygenation phase could reverse the above change. Regain of Ripk3 could significantly alleviated the foci of mitochondria, LC3II and lysosome. **D.** Ripk3 and FUNDC1 interaction was assessed by immunoprecipitation (IP) experiments. *$P < 0.05$ vs the control group, #$P < 0.05$ vs cells in hypoxia condition, &$P < 0.05$ vs the wild-type (WT) group, $$P < 0.05$ vs the Ripk3$^{-/-}$ group.

boosted the number of lysosome containing fragmented mitochondria, and these alterations were suppressed by Ripk3 overexpression. Furthermore, increased LC3II and mitochondria co-localization under Ripk3 deletion in cardiomyocytes (Fig. 3E) and CMECs (Supplemental Fig. 4E) suggested the inhibitory effect of Ripk3 on mitophagy. To verify whether the repressed mitophagy was associated with defective mitochondrial accumulation and apoptosis activation, we used mitophagy activator (FCCP) and inhibitor (3-MA). In cardiomyocytes isolated from Ripk3$^{-/-}$, blockade of mitophagy re-caused cyt-c diffusion into the cytoplasm (Fig. 3F), up-regulated caspase9/3 expression (Fig. 3G-H) and LDH release (Fig. 3I). Instead, mitophagy activation under Ripk3 overexpression could impede mitochondrial apoptosis. Meanwhile, in CMECs, attenuation of mitophagy reduced cell viability (Supplemental Fig. 4F) and increased caspase9 activity (Supplemental Fig. 4G). Thus, on the one hand, these data suggested that mitophagy played an anti-apoptotic role in cardiac IRI through clearing fragmented mitochondria and limiting cyt-c leakage. On the other hand, increased Ripk3 in response to IRI suppressed mitophagy, leading the failure of mitophagy to clear ruptured mitochondria and contributing to an increase in the number of apoptotic cells.

3.4. Ripk3 knockdown reduces infarcted area and improves cardiac and microvasculature function via elevation of mitophagy

To provide further evidence for the anti-apoptotic role of Ripk3 deficiency via mitophagy, animal IRI model was evaluated. Compared with the baseline, Ripk3 depletion significantly reduced the infarct zone (Fig. 4A–B), alleviated cardiac injury marker such as Troponin T and CK-MB (Fig. 4C-D) and improved the cardiac function parameters such as LVEF, LVDd and LVFS (Fig. 4E–H). Nonetheless, blunt mitophagy abated the beneficial effects of Ripk3 deficiency. Structurally, TEM showed the inactivation of mitophagy led to mitochondria injury (red arrow in Fig. 4I), myocyte dissolution, muscular fiber twisting and Z line disappearance (yellow arrow in Fig. 4I) compared with the Ripk3-deficient group. Functionally, Fura-2/AM was used to observe the change of intracellular Ca^{2+} transients in spontaneously beating cardiomyocytes (supplemental video A-D). Fig. 4J showed representative tracings of F340/F380 florescence ratio and Fig. 4K demonstrated that the intracellular resting calcium level was increased in IRI (68.46 ± 6.46 nM in control group and 96.37 ± 9.24 nM in WT group, p < 0.05) but reduced once loss of Ripk3 (74.58 ± 8.53 nM in Ripk3$^{-/-}$ group, p < 0.05 vs. WT group). However, inhibition of mitophagy

under Ripk3$^{-/-}$ caused the rebound of resting calcium (91.27 ± 7.18 nM in 3-MA+Ripk3$^{-/-}$ group, p < 0.05 vs. Ripk3$^{-/-}$ group), suggesting the calcium overload under Ripk3 upregulation or mitophagy inactivation. Fig. 4L showed that the intracellular Ca^{2+} transient amplitude was decreased by 24.15 ± 2.33% under IRI when compared to control group, but it was increased by 21.07 ± 2.58% when loss of Ripk3. Inhibition of mitophagy could alleviate the intracellular Ca^{2+} transient amplitude, suggesting that Ripk3 regulated the cardiomyocytes Ca^{2+}-mediated cellular contraction via mitophagy.

In addition to cardiomyocytes, the microvascular imaging by gelatin-ink perfusion revealed that Ripk3 knockdown sustained the patency of microvessel, which was reduced via the attenuation of mitophagy (Fig. 4M). Structurally, the irregular endothelial swelling and luminal stenosis (red arrow in Fig. 4N) were identified in the cardiac microvessels following IRI in WT mice but not in Ripk3$^{-/-}$ mice via TEM. Blockade of mitophagy in Ripk3$^{-/-}$ mice led to the rebound of microvascular damage. The CEMC migration to infarcted area regenerating vascular network is necessary to repair injured heart. Ripk3 deficiency reversed CEMC mobilization capacity and the balance of mobilization-related proteins such as F-actin/Tubulin under IRI (Fig. 4O), and however, these protective effects were cancelled by mitophagy inhibition.

Supplementary material related to this article can be found online at http://dx.doi.org/10.1016/j.redox.2017.07.007.

3.5. Mitophagy is activated by hypoxia via FUNDC1 but disturbed by Ripk3 in response to reoxygenation

At last, to explore the mechanism through which Ripk3 regulated mitophagy, we focused on FUNDC1-mediated mitophagy. As shown in Fig. 5A–B, FUNDC1 was mainly activated via dephosphorylation (Tyr18) during hypoxia but down-regulated in the period of reoxygenation in isolated cardiomyocytes. Furthermore, through loos- and gain-of function of Ripk3 in vitro, we confirmed the inhibitory role played by Ripk3 in FUNDC1 activation (Fig. 5A–B). Loss of Ripk3 at reoxygenation stage reversed FUNDC1 dephosphorylated activation whereas regain of Ripk3 inhibited FUNDC1 activation regardless of reoxygenation or hypoxia condition. Moreover, the mitochondria, LC3II and lysosome co-staining (Fig. 5C) also supported the restrictive influence of Ripk3 on FUNDC1-required mitophagy via LC3II and lysosome. To further provide the information about the relationship between Ripk3 and FUNDC1, the protein interaction was detected. Our
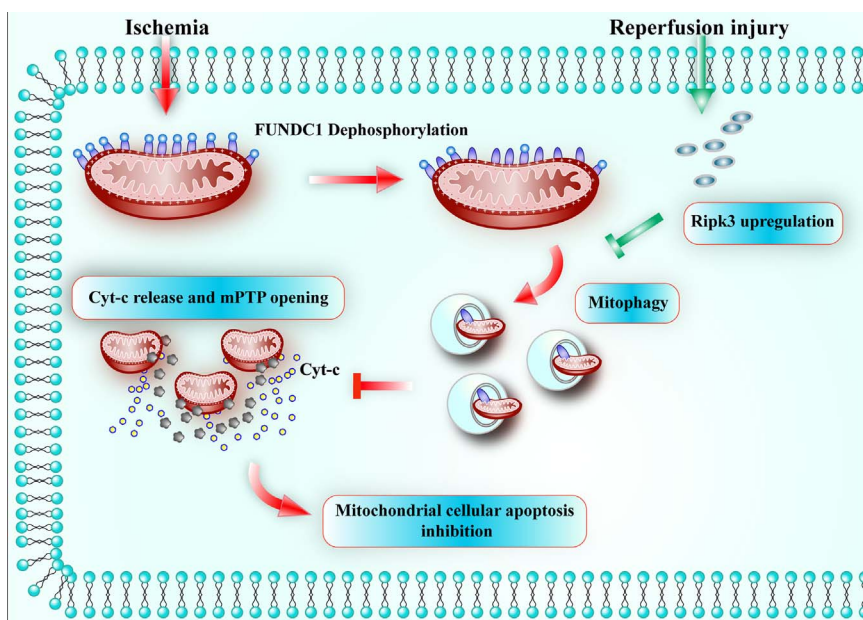

Fig. 6. Under ischemia, FUNDC1 was activated and facilitated mitophagy to selectively degrade the doomed mitochondria and reduce pro-apoptotic factor cyt-c leakage into the cytoplasm, eventually inhibiting caspase9-involved apoptosis. However, after reperfusion, Ripk3 was upregulated, contributing to FUNDC1 deactivation via the post transcriptional modification of the FUNDC1 phosphorylation site. The limited FUNDC1-associated mitophagy failed to eliminate fragmented mitochondria or confine cyt-c diffusion but instead resulted in the caspase9-mediated apoptosis.

results in Fig. 5D shown an interaction between FUNDC1 with Ripk3, suggesting the direct regulatory of Ripk3 on FUNDC1 activation.

4. Discussion

Apoptosis and necroptosis are the dominant types of PCD in the context of IRI and necroptosis is actually the primary cause of death during reperfusion injury according to the latest scientific reports [36,37]. Approximately 50% of cellular death could be blocked through Ripk3 gene deletion, whereas ~ 30% of reperfusion-induced cell death was inhibited by the pan-caspase inhibitor zVAD [37]. Several studies have argued that Ripk3-required necroptosis has multiple functions in apoptosis [38]. In the present study, we observed that Ripk3 contributed to caspase9-mediated mitochondrial apoptosis in response to IRI. Under ischemia, activated FUNDC1 facilitated mitophagy to selectively degrade the doomed mitochondria and reduce pro-apoptotic factor cyt-c leakage into the cytoplasm, eventually inhibiting caspase9-involved apoptosis. However, after reperfusion, Ripk3 was upregulated, contributing to FUNDC1 deactivation via the post transcriptional modification of the FUNDC1 phosphorylation site. The limited FUNDC1-associated mitophagy failed to eliminate fragmented mitochondria or confine cyt-c diffusion but instead resulted in the caspase9-mediated apoptosis of these cells. To our knowledge, we are the first to provide a description of the relationship between Ripk3 and apoptosis in response to cardiac IRI (Fig. 6).

As to the IRI, the regained flow induces oxidative stress outbreak by xanthine oxidase [39] or mitochondria [28], cytoplasmic calcium overload via the calcium-induced calcium release (CICR) process [23] and excessive inflammatory cell infiltration through endothelial hyperpermeability [40]. These changes stimulate Ripk3 via interaction with cellular death receptors, such as TNFR1, FasR, and TRAIL-R [5,6]. In the present study, we illustrated that reperfusion rather than ischemia was the initial signal for Ripk3 activation and the reperfusion-mediated Ripk3 upregulation was implicated in intensive apoptosis. These findings suggested that Ripk3 was the regulatory signal for apoptosis. Indeed, necroptosis and apoptosis undergo multiple interactions with each other. In response to inflammation, the inhibitors of apoptosis (cIAP1 and cIAP2) elicit Ripk1 ubiquitination [41,42], leading to the blockade of necroptosis. By contrast, the amplification of caspase8-dependent apoptosis could cleave and abolish Ripk1/Ripk3 signals, preventing consequent necroptosis [43,44]. However, our data add additional information regarding the interplay of those two types of PCD. Ripk3 could mediate both apoptosis and necrosis which are linked through multiple biochemical and functional associations.

We demonstrated that Ripk3 initiated the caspase9 mitochondrial apoptotic pathway. Because damaged and fragmented mitochondria were rescued by the deletion of Ripk3, we first proposed that Drp1 and subsequent mitochondrial fission was sufficient for Ripk3-mediated apoptosis [45]. However, no variation was observed about Drp1 inactivation with Ripk3 deficiency, deducing that Drp1 was not the subsequent signal of Ripk3. These data provided additional detailed evidence for the role of Ripk3 in Drp1-evoked mitochondrial fission due to the existed controversial related to promotive actions on Drp1 exerted by Ripk3 [46,47]. Recently, accumulating evidence has indicated that both PGAM5 and Drp1 are dispensable for Ripk3/MLKL/necroptosis, and these differences have tissue specificity. As a result, the ubiquity of their involvement in the necroptosis should be examined [48,49].

Although Ripk3 did not prevent the formation of mitochondrial debris in the present study, mitochondrial integrity was more dependent on its tightly complementary degradation systems. One important pathway in this respect is mitophagy [50]. We demonstrated that Ripk3 loss was significantly associated with amplification of FUNDC1-involved mitophagy under IRI. Ample evidences argued that FUNDC1-involved mitophagy was up-regulated during hypoxia [30,51], which was in accordance with our results. However, after reperfusion, Ripk3

was progressively elevated, whereas FUNDC1 and mitophagy was comprehensively perturbed. These synchronously opposite changes suggested a potential link between Ripk3 and FUNDC1-mediated mitophagy. Through protein-interaction assay, we displayed Ripk3 could direct interact with FUNDC1 and inactivate FUNDC-1 as well as mitophagy. Inhibition of mitophagy could cancel the anti-apoptotic effect of Ripk3 deficiency as shown by more fragmented mitochondria, diffused cyt-c leakage, expanded infarcted area and cardiac/microvascular dysfucntion. These data clearly demonstrated that the anti-apoptotic effect of Ripk3 deficiency was attributed to increased mitophagy that is the indispensably important part of the defense system for cells or organs to withstand acute stress challenges [52]. Collectively, deletion of Ripk3 could restore mitophagy responsible for combating apoptosis and our conclusion also hints that the mitophagy is the bridge connecting with mitochondrial apoptosis and Ripk3-required necroptosis. The present study also provides a conclusive view of the interactive influence between Ripk3-required necroptosis, mitochondria-mediated apoptosis and FUNDC1-associated mitophagy. Although the essential action for Ripk3 in mitophagy has been suggested, alternative mechanistic links of mitophagy and necroptosis on the pathogenesis of cardiac reperfusion injury should be illustrated in future studies [53].

In the present study, we not only focused on cardiomyocytes but also investigated microvascular reperfusion injury, which is a neglected topic [54]. Compared to cardiomyocytes, fewer studies have examined the underlying mechanism of microcirculation reperfusion injury [55], and therefore, few strategies are available to reverse such pathologies [56]. The findings of the present study demonstrated that the microvasculature was the primary victim of reperfusion injury and introduced both Ripk3 and mitophagy as underlying pathogenic mechanisms, providing deeper insights into the nature of microcirculatory injury. Because both apoptosis and necroptosis could be terminated though the deletion of Ripk3, the early microvasculature protection potentially targeting Ripk3 to stop the death signal before PCI may be more efficient and beneficial than late salvage treatment during or after PCI [57].

In conclusion, Ripk3-required necroptosis positively regulated mitochondria-mediated apoptosis via FUNDC1 mitophagy. Ischemia activated FUNDC1 and signaled mitophagy to prevent mitochondria-mediated apoptosis, which was repressed by the upregulation of Ripk3 during reperfusion. Ripk3 deletion enhanced anti-apoptotic mitophagy, preventing myocardial and microvascular damage in response to IRI.

Conflict of interest statement

The authors declared that they have no conflicts of interest.

Appendix A. Supplementary material

Supplementary data associated with this article can be found in the online version at http://dx.doi.org/10.1016/j.redox.2017.07.007.

References

[1] R.A. Kloner, C.E. Ganote, R.B. Jennings, The "no-reflow" phenomenon after temporary coronary occlusion in the dog, J. Clin. Investig. 54 (6) (1974) 1496–1508.
[2] D.J. Hausenloy, D.M. Yellon, Ischaemic conditioning and reperfusion injury, Nat.

Rev. Cardiol. 13 (4) (2016) 193–209.

[3] I.M. Dauber, K.M. Vanbenthuysen, I.F. Mcmurtry, G.S. Wheeler, E.J. Lesnefsky, L.D. Horwitz, J.V. Weil, Functional coronary microvascular injury evident as increased permeability due to brief ischemia and reperfusion, Circ. Res. 66 (4) (1990) 986–998.

[4] M.I. Oerlemans, S. Koudstaal, S.A. Chamuleau, D.P. De Kleijn, P.A. Doevendans, J.P. Sluijter, Targeting cell death in the reperfused heart: pharmacological approaches for cardioprotection, Int J. Cardiol. 165 (3) (2013) 410–422.

[5] M.I. Oerlemans, J. Liu, F. Arslan, K. Den Ouden, B.J. Van Middelaar, P.A. Doevendans, J.P. Sluijter, Inhibition of RIP1-dependent necrosis prevents adverse cardiac remodeling after myocardial ischemia-reperfusion in vivo, Basic Res. Cardiol. 107 (4) (2012) 270.

[6] C.C. Smith, S.M. Davidson, S.Y. Lim, J.C. Simpkin, J.S. Hothersall, D.M. Yellon, Necrostatin: a potentially novel cardioprotective agent? Cardiovasc Drugs Ther. 21 (4) (2007) 227–233.

[7] N. Lalaoui, L.M. Lindqvist, J.J. Sandow, P.G. Ekert, The molecular relationships between apoptosis, autophagy and necroptosis, Semin Cell Dev. Biol. 39 (2015) 63–69.

[8] M. Luedde, M. Lutz, N. Carter, J. Sosna, C. Jacoby, M. Vucur, J. Gautheron, C. Roderburg, N. Borg, F. Reisinger, H.J. Hippe, A. Linkermann, M.J. Wolf, S. Rose-John, R. Lullmann-Rauch, D. Adam, U. Flogel, M. Heikenwalder, T. Luedde, N. Frey, RIP3, a kinase promoting necroptotic cell death, mediates adverse remodelling after myocardial infarction, Cardiovasc Res. 103 (2) (2014) 206–216.

[9] J. Zhang, Y. Yang, W. He, L. Sun, Necrosome core machinery: MLKL, Cell Mol. Life Sci. 73 (11–12) (2016) 2153–2163.

[10] K. Newton, RIPK1 and RIPK3: critical regulators of inflammation and cell death, Trends Cell Biol. 25 (6) (2015) 347–353.

[11] A.B. Gustafsson, R.A. Gottlieb, Recycle or die: the role of autophagy in cardioprotection, J. Mol. Cell Cardiol. 44 (4) (2008) 654–661.

[12] G. Meng, G. Xia, D. Wang, A. Chen, Y. Wang, H. Wang, D. Yu, J. Wei, Mitophagy promotes replication of oncolytic Newcastle disease virus by blocking intrinsic apoptosis in lung cancer cells, Oncotarget 5 (15) (2014) 6365–6374.

[13] J.L. Larson-Casey, J.S. Deshane, A.J. Ryan, V.J. Thannickal, A.B. Carter, Macrophage Akt1 kinase-mediated mitophagy modulates apoptosis resistance and pulmonary fibrosis, Immunity 44 (3) (2016) 582–596.

[14] D.A. Kubli, A.B. Gustafsson, Mitochondria and mitophagy: the yin and yang of cell death control, Circ. Res. 111 (9) (2012) 1208–1221.

[15] W. Zhang, H. Ren, C. Xu, C. Zhu, H. Wu, D. Liu, J. Wang, L. Liu, W. Li, Q. Ma, L. Du, M. Zheng, C. Zhang, J. Liu, Q. Chen, Hypoxic mitophagy regulates mitochondrial quality and platelet activation and determines severity of I/R heart injury, Elife 5 (2016).

[16] H. Zhou, Y. Zhang, S. Hu, C. Shi, P. Zhu, Q. Ma, Q. Jin, F. Cao, F. Tian, Y. Chen, Melatonin protects cardiac microvasculature against ischemia/reperfusion injury via suppression of mitochondrial fission-VDAC1-HK2-mPTP-mitophagy axis, J. Pineal Res. (2017).

[17] M.E. Diaz-Casado, E. Lima, J.A. Garcia, C. Doerrier, P. Aranda, R.K. Sayed, A. Guerra-Librero, G. Escames, L.C. Lopez, D. Acuna-Castroviejo, Melatonin rescues zebrafish embryos from the parkinsonian phenotype restoring the parkin/PINK1/DJ-1/MUL1 network, J. Pineal Res. 61 (1) (2016) 96–107.

[18] S. Chen, X. Lv, B. Hu, Z. Shao, B. Wang, K. Ma, H. Lin, M. Cui, RIPK1/RIPK3/MLKL-mediated necroptosis contributes to compression-induced rat nucleus pulposus cells death, Apoptosis 22 (5) (2017) 626–638.

[19] W. Zhang, S. Siraj, R. Zhang, Q. Chen, Mitophagy receptor FUNDC1 regulates mitochondrial homeostasis and protects the heart from I/R injury, Autophagy (2017) 1–2.

[20] Z. Chen, S. Siraj, L. Liu, Q. Chen, MARCH5-FUNDC1 axis fine-tunes hypoxia-induced mitophagy, Autophagy (2017) 1–2.

[21] S. He, L. Wang, L. Miao, T. Wang, F. Du, L. Zhao, X. Wang, Receptor interacting protein kinase-3 determines cellular necrotic response to TNF-alpha, Cell 137 (6) (2009) 1100–1111.

[22] H. Zhou, J. Yang, T. Xin, T. Zhang, S. Hu, S. Zhou, G. Chen, Y. Chen, Exendin-4 enhances the migration of adipose-derived stem cells to neonatal rat ventricular cardiomyocyte-derived conditioned medium via the phosphoinositide 3-kinase/Akt-stromal cell-derived factor-1alpha/CXC chemokine receptor 4 pathway, Mol. Med. Rep. 11 (6) (2015) 4063–4072.

[23] Y. Zhang, H. Zhou, W. Wu, C. Shi, S. Hu, T. Yin, Q. Ma, T. Han, Y. Zhang, F. Tian, Y. Chen, Liraglutide protects cardiac microvascular endothelial cells against hypoxia/reoxygenation injury through the suppression of the SR-Ca(2+)-XO-ROS axis via activation of the GLP-1R/PI3K/Akt/survivin pathways, Free Radic. Biol. Med. 95 (2016) 278–292.

[24] D. Han, W. Huang, X. Li, L. Gao, T. Su, X. Li, S. Ma, T. Liu, C. Li, J. Chen, E. Gao, F. Cao, Melatonin facilitates adipose-derived mesenchymal stem cells to repair the murine infarcted heart via the SIRT1 signaling pathway, J. Pineal Res. 60 (2) (2016) 178–192.

[25] H. Zhou, S. Hu, Q. Jin, C. Shi, Y. Zhang, P. Zhu, Q. Ma, F. Tian, Y. Chen, Mff-dependent mitochondrial fission contributes to the pathogenesis of cardiac microvasculature ischemia/reperfusion injury via induction of mROS-mediated cardiolipin oxidation and HK2/VDAC1 disassociation-involved mPTP opening, J. Am. Heart Assoc. 6 (3) (2017).

[26] S. Wang, X. Zhu, L. Xiong, J. Ren, Ablation of Akt2 prevents paraquat-induced myocardial mitochondrial injury and contractile dysfunction: role of Nrf2, Toxicol. Lett. 269 (2017) 1–14.

[27] H. Zhou, J. Yang, T. Xin, D. Li, J. Guo, S. Hu, S. Zhou, T. Zhang, Y. Zhang, T. Han, Y. Chen, Exendin-4 protects adipose-derived mesenchymal stem cells from apoptosis induced by hydrogen peroxide through the PI3K/Akt-Sfrp2 pathways, Free Radic. Biol. Med 77 (2014) 363–375.

[28] H. Zhou, D. Li, C. Shi, T. Xin, J. Yang, Y. Zhou, S. Hu, F. Tian, J. Wang, Y. Chen, Effects of Exendin-4 on bone marrow mesenchymal stem cell proliferation, migration and apoptosis in vitro, Sci. Rep. 5 (2015) 12898.

[29] J. Wei, H. Xu, L. Shi, J. Tong, J. Zhang, Trimetazidine protects cardiomyocytes

[30] G. Chen, Z. Han, D. Feng, Y. Chen, L. Chen, H. Wu, L. Huang, C. Zhou, X. Cai, C. Fu, L. Duan, X. Wang, L. Liu, X. Liu, Y. Shen, Y. Zhu, Q. Chen, A regulatory signaling loop comprising the PGAM5 phosphatase and CK2 controls receptor-mediated mitophagy, Mol. Cell 54 (3) (2014) 362–377.

[31] W. Wu, W. Tian, Z. Hu, G. Chen, L. Huang, W. Li, X. Zhang, P. Xue, C. Zhou, L. Liu, Y. Zhu, X. Zhang, L. Li, L. Zhang, S. Sui, B. Zhao, D. Feng, ULK1 translocates to mitochondria and phosphorylates FUNDC1 to regulate mitophagy, EMBO Rep. 15 (5) (2014) 566–575.

[32] N. Prieto-Dominguez, R. Ordonez, A. Fernandez, C. Mendez-Blanco, A. Baulies, C. Garcia-Ruiz, J.C. Fernandez-Checa, J.L. Mauriz, J. Gonzalez-Gallego, Melatonin-induced increase in sensitivity of human hepatocellular carcinoma cells to sorafenib is associated with reactive oxygen species production and mitophagy, J. Pineal Res. 61 (3) (2016) 396–407.

[33] J. Zhang, Teaching the basics of autophagy and mitophagy to redox biologists–mechanisms and experimental approaches, Redox Biol. 4 (2015) 242–259.

[34] S.W. Ryter, A.M. Choi, Autophagy in lung disease pathogenesis and therapeutics, Redox Biol. 4 (2015) 215–225.

[35] H.M. Ni, J.A. Williams, W.X. Ding, Mitochondrial dynamics and mitochondrial quality control, Redox Biol. 4 (2015) 6–13.

[36] J.X. Wang, X.J. Zhang, Q. Li, K. Wang, Y. Wang, J.Q. Jiao, C. Feng, S. Teng, L.Y. Zhou, Y. Gong, Z.X. Zhou, J. Liu, J.L. Wang, P.F. Li, MicroRNA-103/107 regulate programmed necrosis and myocardial ischemia/reperfusion injury through targeting FADD, Circ. Res. 117 (4) (2015) 352–363.

[37] T. Zhang, Y. Zhang, M. Cui, L. Jin, Y. Wang, F. Lv, Y. Liu, W. Zheng, H. Shang, J. Zhang, M. Zhang, H. Wu, J. Guo, X. Zhang, X. Hu, C.M. Cao, R.P. Xiao, CaMKII is a RIP3 substrate mediating ischemia- and oxidative stress-induced myocardial necroptosis, Nat. Med. 22 (2) (2016) 175–182.

[38] A. Ashkenazi, G. Salvesen, Regulated cell death: signaling and mechanisms, Annu. Rev. Cell Dev. Biol. 30 (2014) 337–356.

[39] Proceedings of the joint summer meeting of the British and American Neuropsychiatry Associations, 12–14 July, Oxford, J. Neurol. Neurosurg. Psychiatry vol. 55(11), 1992, pp. 1098–1100.

[40] D.J. Marchant, J.H. Boyd, D.C. Lin, D.J. Granville, F.S. Garmaroudi, B.M. Mcmanus, Inflammation in myocardial diseases, Circ. Res. 110 (1) (2012) 126–144.

[41] M.J. Bertrand, S. Milutinovic, K.M. Dickson, W.C. Ho, A. Boudreault, J. Durkin, J.W. Gillard, J.B. Jaquith, S.J. Morris, P.A. Barker, cIAP1 and cIAP2 facilitate cancer cell survival by functioning as E3 ligases that promote RIP1 ubiquitination, Mol. Cell 30 (6) (2008) 689–700.

[42] D. M. A. O'donnell, P. Legarda-Addison, W.C. Skountzos, A.T. Yeh, Ting, Ubiquitination of RIP1 regulates an NF-kappaB-independent cell-death switch in TNF signaling, Curr. Biol. 17 (5) (2007) 418–424.

[43] W.J. Kaiser, H. Sridharan, C. Huang, P. Mandal, J.W. Upton, P.J. Gough, C.A. Sehon, R.W. Marquis, J. Bertin, E.S. Mocarski, Toll-like receptor 3-mediated necrosis via TRIF, RIP3, and MLKL, J. Biol. Chem. 288 (43) (2013) 31268–31279.

[44] C.P. Dillon, A. Oberst, R. Weinlich, L.J. Janke, T.B. Kang, T. Ben-Moshe, T.W. Mak, D. Wallach, D.R. Green, Survival function of the FADD-CASPASE-8-cFLIP(L) complex, Cell Rep. 1 (5) (2012) 401–407.

[45] D.N. Granger, P.R. Kvietys, Reperfusion injury and reactive oxygen species: the evolution of a concept, Redox Biol. 6 (2015) 524–551.

[46] D.M. Moujalled, W.D. Cook, J.M. Murphy, D.L. Vaux, Necroptosis induced by RIPK3 requires MLKL but not Drp1, Cell Death Dis. 5 (2014) e1086.

[47] Q. Remijsen, V. Goossens, S. Grootjans, C. Van Den Haute, N. Vanlangenakker, Y. Dondelinger, R. Roelandt, I. Bruggeman, A. Goncalves, M.J. Bertrand, V. Baekelandt, N. Takahashi, T.V. Berghe, P. Vandenabeele, , Depletion of RIPK3 or MLKL blocks TNF-driven necroptosis and switches towards a delayed RIPK1 kinase-dependent apoptosis, Cell Death Dis. 5 (2014) e1004.

[48] J.M. Murphy, P.E. Czabotar, J.M. Hildebrand, I.S. Lucet, J.G. Zhang, S. Alvarez-Diaz, R. Lewis, N. Lalaoui, D. Metcalf, A.I. Webb, S.N. Young, L.N. Varghese, G.M. Tannahill, E.C. Hatchell, I.J. Majewski, T. Okamoto, R.C. Dobson, D.J. Hilton, J.J. Babon, N.A. Nicola, A. Strasser, J. Silke, W.S. Alexander, The pseudokinase MLKL mediates necroptosis via a molecular switch mechanism, Immunity 39 (3) (2013) 443–453.

[49] B. Schenk, S. Fulda, Reactive oxygen species regulate Smac mimetic/TNFalpha-induced necroptotic signaling and cell death, Oncogene 34 (47) (2015) 5796–5806.

[50] F. Nduhirabandi, K. Lamont, Z. Albertyn, L.H. Opie, S. Lecour, Role of toll-like receptor 4 in melatonin-induced cardioprotection, J. Pineal Res. 60 (1) (2016) 39–47.

[51] L. Liu, D. Feng, G. Chen, M. Chen, Q. Zheng, P. Song, Q. Ma, C. Zhu, R. Wang, W. Qi, L. Huang, P. Xue, B. Li, X. Wang, H. Jin, J. Wang, F. Yang, P. Liu, Y. Zhu, S. Sui, Q. Chen, Mitochondrial outer-membrane protein FUNDC1 mediates hypoxia-induced mitophagy in mammalian cells, Nat. Cell Biol. 14 (2) (2012) 177–185.

[52] J. Dan Dunn, L.A. Alvarez, X. Zhang, T. Soldati, Reactive oxygen species and mitochondria: a nexus of cellular homeostasis, Redox Biol. 6 (2015) 472–485.

[53] K. Mizumura, S.M. Cloonan, K. Nakahira, A.R. Bhashyam, M. Cervo, T. Kitada, K. Glass, C.A. Owen, A. Mahmood, G.R. Washko, S. Hashimoto, S.W. Ryter, A.M. Choi, Mitophagy-dependent necroptosis contributes to the pathogenesis of COPD, J. Clin. Investig. 124 (9) (2014) 3987–4003.

[54] G. Heusch, Cardioprotection: chances and challenges of its translation to the clinic, Lancet 381 (9861) (2013) 166–175.

[55] G. Heusch, The coronary circulation as a target of cardioprotection, Circ. Res. 118 (10) (2016) 1643–1658.

[56] G. Niccoli, G. Scalone, A. Lerman, F. Crea, Coronary microvascular obstruction in acute myocardial infarction, Eur. Heart J. 37 (13) (2016) 1024–1033.

[57] R. Jaffe, A. Dick, B.H. Strauss, Prevention and treatment of microvascular obstruction-related myocardial injury and coronary no-reflow following percutaneous coronary intervention: a systematic approach, JACC Cardiovasc. Interv. 3 (7) (2010) 695–704.